Journal of the European Ceramic Society 22 (2002) 2963–2968

www.elsevier.com/locate/jeurceramsoc

Polysilazane derived micro/nano Si_3N_4/SiC composites

Matilda Zemanová[a,*], Emmanuel Lecomte[b], Pavol Šajgalík[c], Ralf Riedel[b]

[a]*Faculty of Chemical Technology Slovak University of Technology, Department of Inorganic Technology, Radlinského 9, SK-812 37 Bratislava, Slovakia*
[b]*FG Disperse Feststoffe, FB Materialwissenschaft, Technische Universität Darmstadt, Petersenstr. 23, D-64287 Darmstadt, Germany*
[c]*Institute of Inorganic Chemistry Slovak Academy of Sciences, Dúbravská cesta 9, SK-842 36 Bratislava, Slovakia*

Received 10 January 2001; received in revised form 24 January 2002; accepted 24 February 2002

Abstract

The pyrolised polysilazanes poly(hydridomethyl)silazane NCP 200 and poly(urea)silazane CERASET derived Si–C–N amorphous powders were used for preparation of micro/nano Si_3N_4/SiC composites by hot pressing. Y_2O_3–Al_2O_3 and Y_2O_3–Yb_2O_3 were used, as sintering aids. The resulting ceramic composites of all compositions were dense and polycrystalline with fine microstructure of average grain size <1 μm of both Si_3N_4 and SiC phases. The fine SiC nano-inclusions were identified within the Si_3N_4 micrograins. Phase composition of both composites consist of α, β modifications of Si_3N_4 and SiC. High weight loss was observed during the hot pressing cycle, 12 and 19 wt.% for NCP 200 and CERASET precursors, respectively. The fracture toughness of both nanocomposites (NCP 2000 and CERASET derived) was not different. Indentation method measured values are from 5 to 6 MPa $m^{1/2}$, with respect to the sintering additive system. Fracture toughness is slightly sensitive to the SiC content of the nanocomposite. Hardness increases with the content of SiC in the nanocomposite. The highest hardness was achieved for pyrolysed CERASET precursor with 2 wt.% Y_2O_3 and 6 wt.% Yb_2O_3, HV $\cong$ 23 GPa. This is a consequence of the highest SiC content as well as the chemical composition of additives.

Keywords: Precursors-organic; Si_3N_4/SiC; Composites; Microstructure-final; Hardness; Toughness; Phase development

1. Introduction

Recently developed Si_3N_4/SiC composites belong to the family of advanced materials because of their outstanding mechanical properties and corrosion resistance at high temperatures.[1–3] These composites consist of Si_3N_4 micro-grains and SiC nano-inclusions, which are located within the host Si_3N_4 grains and along their grain boundaries. Enhanced room as well as high temperature properties are reported for nano/micro composites prepared by hot-pressing of CVD SiNC amorphous powder. Hot-pressing or gas pressure sintering of mechanical mixture of sub-micrometer crystalline Si_3N_4 and SiC powders are the other reported ways used for processing of nano/micro composites.[4,5] In such a way prepared composites have not reached the properties of the CVD derived materials.

Another reported processing method is a compromise between both above mentioned approaches, the nano/micro composites were prepared by adding polymer derived amorphous Si–C–N powder into the crystalline Si_3N_4 starting mixture.[6] The room and high temperature mechanical properties of Si_3N_4/SiC composite materials were enhanced in comparison to the relative monoliths.

The next intensively studied processing method is using amorphous polysilazane derived starting Si–C–N powder, which is converted to a sintered body of fine crystals by hot pressing with sintering additives in a nitrogen atmosphere.[7] Amorphous Si–C–N starting powder has been prepared by the pyrolysis of organo-substituted polysilazanes ($[–RSiR'–NH–]_n$, where R is H or CH_3 and R′ is CH_3) under protective argon atmosphere. Owing to the covalent nature of the Si–C and Si–N bonds and hence the low diffusion coefficients, additions of oxides were used in order to obtain a dense ceramic body.[8] The sintering additives are in principle selected on the basis of known phase diagrams[9] with the aim to prepare a high viscous grain boundary phase at high temperatures.

The present work is using the last mentioned processing method with the aim to investigate the sinterability of amorphous starting powders derived from organo-

* Corresponding author.

0955-2219/02/$ - see front matter
PII: S0955-2219(02)00039-0

metallic precursors. Two different types of precursors were used in this study, NCP 200 and CERASET. Some experiences with sintering of NCP200 derived powders were already published,[10] the CERASET derived powders are used for the first time. The data on densification behaviour, phase composition, fracture toughness and hardness of the dense Si_3N_4/SiC nanocomposites are presented.

2. Experimental

The precursor polysilazane CERASET is a liquid very sensitive to the moisture and oxygen. Therefore a polysilazane polymer was manipulated and stored in a glove box under argon of 99.999% purity (Linde AG, Germany). The 20 g of polysilazane was filled into a quartz tube and pyrolysed in a vertical quartz tube furnace with SiC heating elements (Gero, model HTSR 40–2000, temperature measured by Pt-PtRh10 thermocouple). The precursor was heat treated at 1000°C for one hour. Amorphous Si–C–N powder was prepared. The precursor NCP 200 (Nichimen Corporation, Japan) is a powder. The pyrolysis temperature profile for NCP 200 is different comparing to the pyrolysis of liquid CERASET. NCP 200 was first cross-linked at 350 °C for 2 h and subsequently pyrolysed at 1100 °C for 1 h. The storage conditions and manipulation were similar to CERASET precursor.

The amorphous Si–C–N powder together with Y_2O_3–Al_2O_3/Y_2O_3–Yb_2O_3 sintering additives were homogenised in hexan by Si_3N_4 balls in teflon 1 l pot mill for 15 h. The dried starting mixture was then compacted to the pellets of 2 cm in diameter. All samples were densified by hot pressing (KCE 8015, Rödental, model HPW 150) at 1800 °C for 2 h at load of 25 MPa in a flowing N_2 atmosphere. Densification of the samples during a hot pressing cycle was recorded by a dilatometer. Specimens powdered in an agate mortar pot were used for crystalline phase characterisation by X-ray diffraction (XRD) using a Siemens D5000 (CuK_α radiation) difractometer operating at 25 kV. Raman spectra were measured using a double monochromator Ramanor U-1000 (Joben-Yvon, France) equipped with a photomultiplier R 3310–02 (Hamamatsu, Japan). Hot pressed specimens were ground and polished down to 1 μm using the Struers polishing equipment Phoenix 4000. The microstructures were examined by SEM (Philips SEM model VL 30FEG) on polished and plasma etched specimens surface.

The bulk densities were determined by water immersion method. No open porosity/macro pores were observed on samples hot pressed with the sintering additives. Hardness measurements were performed by Vickers indenter at load of 98 N for 10 s. Fracture toughness was estimated by the indentation method using the Equation of Shetty.[11] We analysed the ceramics for its C content by analyser Leco C-200 (Leco Corp. St. Joseph, MI, USA). At the assumption of the total consumption of C at the SiC formation and at the assumption of the mixture formation we calculated the weight percentage of SiC.

3. Results and discussion

3.1. Densification behaviour

The dense nano composite ceramics on the basis of CERASET and NCP 200 polysilazane with sintering additives were prepared by hot pressing in nitrogen flowing atmosphere at 1800 °C for 2 h. The compositions, densities, weight loss, hardness and fracture toughness are listed in Table 1. The shape of shrinkage curves of polysilazane derived composites (Fig. 1) during hot pressing are similar to those of densification curves of hot pressed conventional crystalline powders. On the other hand, the extension of shrinkage is substantially different, shrinkage of amorphous Si–C–N powders is very high comparing to the crystalline powders.

As it can be seen from Fig. 1 the densification is quite intense for the first 50 min. After 50 min the shrinkage rate slows down till it reaches the plateau. The shrinkage of starting composition derived from CERASET (CII) is more intense, total shrinkage is 70% for this precursor comparing to the starting mixture derived from NCP 200 (NII) which is 60%. Densification process is accompanied by a substantial weight loss, Table 1. Difference in shrinkage between both CII and NII materials is probably a consequence of the fact that weight loss of CII composite is almost 1.5–2 times

Table 1
The density, hardness and fracture toughness of Si_3N_4/SiC composite in dependence on starting material composition

Composition	Label	ρ (g cm^{-3})	Weight loss (%)	HV (GPa)	K_{IC} (MPa m$^{1/2}$)
CERASET + 5 Y_2O_3 + 3 Al_2O_3	CI	3.26	19.0	20.2±0.9	5.0±0.2
CERASET + 6 Yb_2O_3 + 2 Y_2O_3	CII	3.39	19.0	22.8±1.1	6.1±0.3
NCP + 5Y_2O_3 + 3Al_2O_3	NI	3.24	11.8	18.2±0.8	5.2±0.1
NCP + 6Yb_2O_3 + 2Y_2O_3	NII	3.33	9.9	22.1±1.0	6.2±0.4

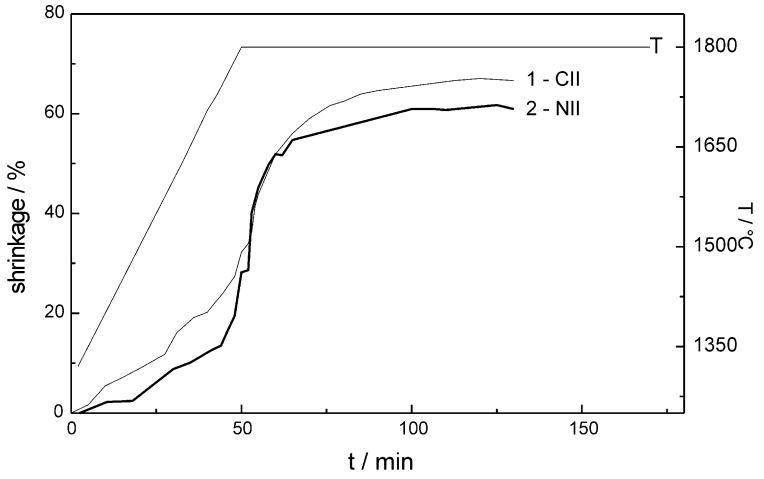

Fig. 1. The densification curves of nanocomposites derived from CERASET + 6 wt.% Yb_2O_3 + 2 wt.% Y_2O_3 (CII) and NCP200 + 6 wt.% Yb_2O_3 + 2 wt.% Y_2O_3 (NII).

higher than NII at the same conditions of hot pressing. The weight loss of CII material is approx. 19%, while for NII a weight loss is approx. 10%. Usual weight loss of Si_3N_4 based composites prepared from a crystalline powder is almost 10 times smaller, usually not higher than 1–3 wt.%. The high weight loss of amorphous starting powder could cause a change of the local chemistry. It is important to keep a distribution of chemical constituents and their ratio in the final composite in order to reach the designed phase composition and microstructure characteristics.

3.2. Phase composition

The XRD records of CII and NII samples show peaks belonging to α-Si_3N_4, α and β phases of SiC and β-Si_3N_4 phase is also recorded in the smaller extent, Fig. 2. The Raman spectrum of CI sample shown in Fig. 3 confirms this statement. The Raman spectrum of CI composite is shown together with the Raman spectrum of the hot pressed sample on the basis of CERASET derived starting powder without sintering additives. The pattern of the sample marked 1 and belonging to the sample prepared on the Ceraset basis without sintering additives shows besides an α-SiC phase peak at 900 cm^{-1} and β-SiC peak at 780 cm^{-1}, also a free carbon peak at approx. 1500 cm^{-1}. CI composition contains phases α and β of SiC and Si_3N_4, but no free carbon. The same observation was confirmed also for the NCP 200 derived composites. This result is very important because of the fact, that the pyrolised powders NCP 200 and CERASET contained 6.3 and 3.9 wt.% of free carbon, respectively.[10] Free carbon in starting powder reacted with silicon dioxide, present as an impurity in the Si–C–N amorphous powder and volatile CO escapes during the hot-pressing cycle. This is one of the reasons of high weight loss of the polysilazane derived nanocomposites.

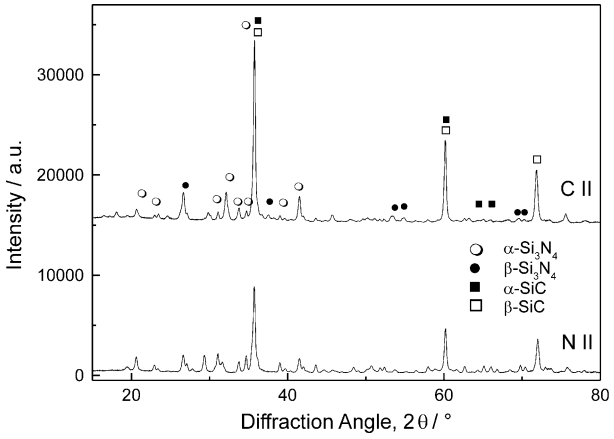

Fig. 2. The XRD patterns of nanocomposites derived from CERASET + 6 wt.% Yb_2O_3 + 2 wt.% Y_2O_3 (CII) and NCP200 + 6 wt.% Yb_2O_3 + 2 wt.% Y_2O_3 (NII).

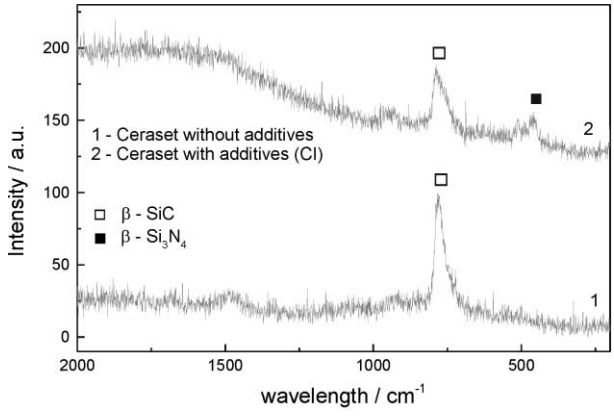

Fig. 3. The Raman spectra of nanocomposite derived from CERASET precursor + 5 wt.% Y_2O_3 + 3 wt.% Al_2O_3 (C I) and a reference spectra of CERASET hot pressed without additives.

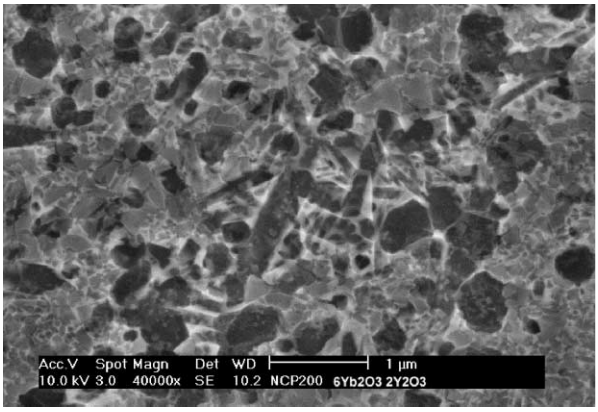

Fig. 4. The SEM picture of Si_3N_4/SiC nanocomposite derived from NCP 200 + 6 wt.% Yb_2O_3 + 2 wt.% Y_2O_3 (NII).

3.3. Microstructure

The SEM micrographs of NII and CII compositions are shown in Figs. 4 and 5, respectively. As it can be seen from Figs. 4 and 5, nanocomposites Si_3N_4/SiC obtained from polysilazanes NCP 200 and Ceraset with additives have comparable microstructure. The needle-like shape is typical for the β-Si_3N_4 phase and the irregular shape of grains is recognised as the α-Si_3N_4 phase. The microstructure of CII composite, Fig. 6, is soft and formed especially by the SiC and glassy phases with island-shaped parts of the Si_3N_4 crystals (Si_3N_4 grains are etched out in contrary to the SiC grains). These Si_3N_4 parts indicate the crystallised areas of crystalline Si_3N_4 phase from the supersaturated oxi-carbo-nitride melt during hot-pressing. At higher magnification, as we can see from Fig. 7, the SiC nanoinclusions are crystallised on the surface of the Si_3N_4 grains. According to Niihara[1] classification it can be assumed that an Inter/Intra type of formed micro/nano Si_3N_4/SiC composite was obtained, which conclusion is in agreement with results of other authors.[4,12]

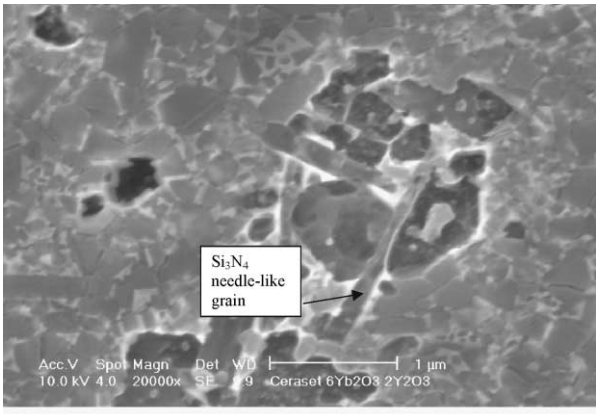

Fig. 5. The SEM picture of Si_3N_4/SiC nanocomposite derived from CERASET + 6 wt.% Yb_2O_3 + 2 wt.% Y_2O_3 (CII).

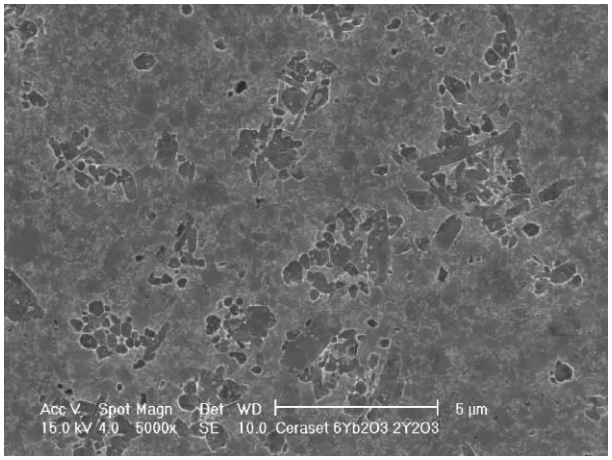

Fig. 6. The SEM micrograph of Si_3N_4/SiC composite prepared from CERASET + 6 wt.% Yb_2O_3 + 2 wt.% Y_2O_3 (CII).

3.4. Hardness and fracture toughness

Table 2 summarises the literature data together with the values of hardness and fracture toughness of nanocomposites prepared in the present work. Data are arranged according to the increasing SiC content. The NII composite reaches relatively high values of fracture toughness and hardness, 6.2 MPa $m^{1/2}$ and 22 GPa, respectively. The CII composite reaches the comparable qualities, $K_{IC} \cong 6$ M Pa $m^{1/2}$, and HV ≅ 23 GPa, respectively. The NI and CI composites reached systematically lower values of fracture toughness and hardness, comparing to those of NII and CII, Table 2. An important conclusion drawn from this fact is that replacement of Al_2O_3 by Yb_2O_3 in the additive system increased the hardness of the nanocomposite. The difference in fracture toughness of two additive systems is also observable, but not significant.

Fig. 8 shows the influence of the SiC content and sintering additive composition on the hardness and fracture toughness. The general tendency that the hardness increases with the increase of SiC content is clearly visi-

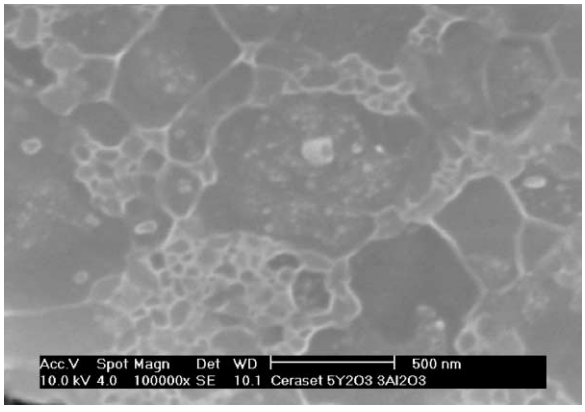

Fig. 7. SiC nanoinclusions within the Si_3N_4 micrograins in CERASET + 5 wt.% Yb_2O_3 + 3 wt.% Y_2O_3 (CI) derived composite.

Table 2
Hardness and fracture toughness of Si_3N_4 based composites with respect to the SiC content

Sample	SiC content (wt.%)	Hardness HV10 (GPa)	Fracture toughness (MPa $m^{1/2}$)	Ref.
92SN 5Y3Al[a]	0	13.5	6.1	14
78SN5Y3Al[b]	7	15.5	5.8	8
56SN5Y3Al[c]	15	16.2	5.8	8
NI	42	18.2	5.2	[d]
NII	45	22.1	6.2	[d]
CI	58	20.2	5.0	[d]
CII	60	22.8	6.1	[d]

[a] 92 wt.% Crystalline Si_3N_4 + 4.6 wt.% Y_2O_3 + 3.4 wt.% Al_2O_3.
[b] 78 wt.% Crystalline Si_3N_4 + 5 wt.% Y_2O_3 + 3 wt.% Al_2O_3 + 14 wt.% amorphous Si–C–N.
[c] 56 wt.% Crystalline Si_3N_4 + 5 wt.% Y_2O_3 + 3 wt.% Al_2O_3 + 36 wt.% amorphous Si–C–N.
[d] This work.

ble from Fig. 8. This conclusion is fully in agreement with the nature of SiC and Si_3N_4 single crystals and the results of other authors.[13,14] Fracture toughness is constant or slightly decreases with the SiC content increase.

Based on these results it can be concluded that there are two factors that influence hardness of precursor derived SiC/Si_3N_4 nano-composites:

- SiC content, and
- Chemistry of the additive system.

This conclusion is in agreement with the general view on the ceramic polycrystalline materials. Hardness is related to the size/area of Vickers imprint. Vickers indenter at the load of 98 N caused imprints of size about 30–40 μm. This size is much larger as than the size of individual micrograin and thus, the calculated hardness value definitely reflects the good quality (in this case hardness/strength) of the grain boundary. The same is valid for the fracture toughness, where the toughening mechanisms are strongly dependent on the grain boundary chemistry.[13] Usually decrease of Al_2O_3 content increases the fracture toughness.

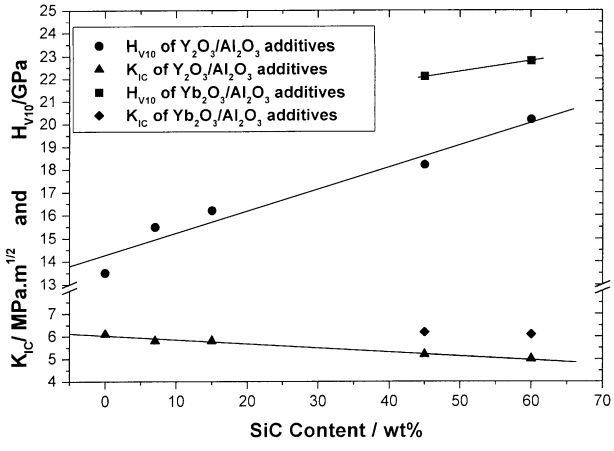

Fig. 8. Hardness and fracture toughness of Si_3N_4–SiC based composites with respect to the SiC content and additive system.

Generally, hardness of silicon nitride-based composite is also dependent on the ratio of α/β-Si_3N_4 phase in the densified sample. The final composition of both precursor-derived materials contained peaks of α-Si_3N_4 phase, Fig. 2. In the present case, the grain boundary composition and high content of the SiC phase probably enhanced this effect.

4. Conclusions

The dense CERASET and NCP 200 derived micro/nano Si_3N_4/SiC composites were prepared by hot pressing in flowing nitrogen atmosphere at 1800 °C and mechanical load of 25 MPa for 2 h. To obtain a dense ceramic body the Y_2O_3–Al_2O_3 and Y_2O_3–Yb_2O_3 additive systems were used. α/β-Si_3N_4 as well as α/β-SiC phases were identified in the resulting nanocomposite. Free carbon present in the starting amorphous Si–C–N powders was not detected in the dense composite. Fracture toughness of nanocomposites derived from both precursor types is similar. Hardness of CERASET derived nanocomposite is slightly higher comparing to NCP 200 because of higher SiC content in the resulting composite. The additive system plays an important role with respect to hardness and fracture toughness. Nanocomposites of both precursors with the Y_2O_3–Yb_2O_3 additives expose higher hardness and fracture toughness compared to those prepared with Y_2O_3–Al_2O_3 additive system.

Acknowledgements

Present work was partly supported by the DAAD, Bonn, Slovak–German R&D Program, project X292.11 and Slovak Grant Agency VEGA, under the project No. 2/5118/00.

References

1. Niihara, K., New design concept of structural ceramics—ceramic nanocomposites. *J. Jpn. Ceram. Soc.*, 1991, **99**(10), 974–982.
2. Rendtel, A., Hübner, H., Herrmann, M. and Schubert, C., Silicon nitride/silicon carbide nanocomposite materials: II, hot strength, creep, and oxidation resistance. *J. Am. Ceram. Soc.*, 1998, **81**(5), 1109–1120.
3. Šajgalík, P., Hnatko, M., Lofaj, F., Hvizdoš, P., Dusza, J., Warbichler, P., Hofer, F., Riedel, R., Lecomte, E. and Hoffmann, M. J., SiC/Si_3N_4 nano/micro-composites- processing, rt and ht mechanical properties. *J. Eur. Ceram. Soc.*, 2000, **20**(4), 453–462.
4. (A) Sasaki, G., Nakase, H., Suganuma, K., Fujita, T. and Niihara, K., Mechanical properties and microstructure of Si_3N_4 matrix composite with nano-meter scale SiC particles. *J. Ceram. Soc. Jpn.* 1992, **100**(4), 536–540. (B) Sasaki, G., Suganuma, K.,

Fujita, T., Hiraga, K. and Niihara, K., Interface structure of Si_3N_4 matrix composite with nano-meter scale SiC particles. *Mar. Res. Symp. Proc.* 1993, **287**, 335–340.
5. Herrmann, M., Schubert, C., Rendtel, A. and Hübner, H., Silicon nitride/silicon carbide nanocomposite materials: I, fabrication and mechanical properties at room temperature. *J. Am. Ceram. Soc.*, 1998, **81**(5), 1094–1108.
6. Šajgalík, P., Hnatko, M. and Lenèéš, Z., Silicon nitride/carbide nano/micro composites for room as well as high temperature applications. *Key Engineering Materials*, 2000, **175–176**, 289–300.
7. Riedel, R., Seher, M. and Becker, G., Sintering of amorphous polymer-derived Si, N and C containing composite powders. *J. Eur. Ceram. Soc.*, 1989, **5**, 113–122.
8. Riedel, R., Passing, G., Schönfelder, H. and Brook, R. J., Synthesis of dense silicon-based ceramics at low temperatures. *Nature*, 1992, **355**, 714.
9. McHale, A. E. (ed.), *Phase Diagrams for Ceramists, Vol. X, Borides, Carbides and Nitrides*. NIST, The American Ceramic Society, Westerville, OH, 1994.
10. Lecomte, E., Riedel, R. and Šajgalík, P., Herstellung und Charakterisierung von aus Polzsilayan-abgeleiteten Si_3N_4/SiC Verbundwerkstoffen. In *Werkstoffwoche, Band VII Keramik*, ed. J. Heinrich, G. Ziegler, W. Hermel and H. Riedel. Wiley-VCH, Weinheim, New York, Chichester, Brisbane, Singapore, Toronto, 1999, pp. 37–42.
11. Shetty, D. K., Wright, I. G., Mincer, P. M. and Clauer, A. H., Indentation fracture of WC-Co cermets. *J. Mater. Sci.*, 1985, **20**, 1873–1882.
12. Hirano, T., Nakahira, A., Niihara, K., Izaki, K., Wakai, F. and Ohji, T., Advances in ceramix matrix composites II. In *Ceramic Trans., Vol. 46*, ed. J. P. Singh and N. P. Bansal, 1994, pp. 519–530.
13. Becher, P. In *Engineering Ceramics '96: Higher Reliability through Processing*. ed. G. N. Babini, M. Haviar, P. Šajgalík, Kluwer Academic, Dordrecht/Boston/London, 1997, pp. 301–310.
14. Šajgalík, P. and Dusza, J., Preparation and properties of fine Si_3N_4 ceramics. *Key Engineering Materials*, 1994, **89–91**, 171–174.